A molecular-engineered rotaxane overcomes longstanding biofluid-challenges and enables optical tryptophan detection in human serum

Joana Krämer[a], Laura M. Grimm[a], Chunting Zhong[a,b], Michael Hirtz[a,b], and Frank Biedermann[a]*

[a] *Institute of Nanotechnology (INT), Karlsruhe Institute of Technology (KIT), Hermann-von-Helmholtz Platz 1, 76344 Eggenstein-Leopoldshafen, Germany*

[b] *Karlsruhe Nano Micro Facility (KNMFi), Karlsruhe Institute of Technology (KIT), Hermann-von-Helmholtz Platz 1, 76344 Eggenstein-Leopoldshafen, Germany*

1. Experimental section

a. Materials

All chemicals and analytes used were purchased from MERCK, TCI, SIGMA ALDRICH, ACROS ORGANICS, and ALFA AESAR and used without further purification with at least the quality label "for synthesis". Dry solvents were stored over molecular sieves (3 Å or 4 Å) to ensure their aridity over long periods. Deuterated solvents were purchased from VWR CHEMICALS and ACROS ORGANICS. Buffer solutions were prepared following standard protocols. For 1X PBS, buffer tablets from CRUZ CHEM were dissolved in 500 mL ultrapure water and no further pH adjustment was carried out. Blood serum samples were purchased from MERCK, SEQENS, and CYTIVA. Pepsin (from porcine gastric mucosa powder) was purchased from SIGMA ALDRICH and bovine serum albumin (BSA) from BIOWEST.

Concentrations of stock solutions were determined by UV-Vis titration measurements based on their extinction coefficients (dopamine: $\varepsilon_{280nm} = 2670\ M^{-1}\ cm^{-1}$;[1] IAA: $\varepsilon_{280nm} = 6000\ M^{-1}\ cm^{-1}$;[2] indole: $\varepsilon_{278nm} = 5670\ M^{-1}\ cm^{-1}$;[3] MDAP: $\varepsilon_{393nm} = 7800\ M^{-1}\ cm^{-1}$; L-Phe: $\varepsilon_{257nm} = 195\ M^{-1}\ cm^{-1}$;[4] tryptamine: $\varepsilon_{279nm} = 5660\ M^{-1}\ cm^{-1}$;[5] L-Trp: $\varepsilon_{279nm} = 5590\ M^{-1}\ cm^{-1}$ [6]).

b. Synthetic procedures

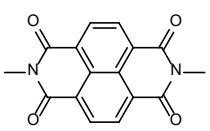

2,7-Dimethylbenzo[*lmn*][3,8]phenanthroline-1,3,6,8(2H,7H)-tetraone[7] (2): A three-neck flask equipped with a reflux condenser was filled with 120 mL aqueous methylamine (40.0 wt%, 1.39 mol, 74.6 eq) and 5.00 g of 1,4,5,8-naphtalenetetracarboxylic dianhydride (18.6 mmol, 1.00 eq) were slowly added under vigorous stirring. The orange-brown solution was refluxed for 3 h, cooled down to room temperature, and stirred for 2 days. The formed precipitate was collected by filtration, washed with copious amounts of methanol and dried *in vacuo*. The product was isolated as a nude-colored solid with a yield of 3.09 g (10.5 mmol, 55.6%).
^{1}H NMR (500 MHz, chloroform-d_1): δ 8.78 (s, 4H, *H*-Ar), 3.61 ppm (s, 6H, CH_3); ^{13}C NMR (126 MHz, chloroform-d_1): δ 163.3 (C_q), 131.15 (C_q), 126.8 (C_q), 126.8 (CH), 27.6 ppm (CH_3).

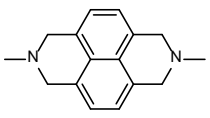

2,7-Dimethyl-1,2,3,6,7,8-hexahydrobenzo[*lmn*][3,8]phenanthroline[8] (3): A 250 ml three-neck flask was loaded with 5.30 g of anhydrous $AlCl_3$ (39.8 mmol, 2.34 eq) which were suspended in 250 mL dry THF. Under ice bath cooling, 4.50 g of $LiAlH_4$ (120 mmol, 7.05 eq) were added stepwise to the stirring suspension. Past the slow addition of 5.00 g of 2,7-dimethylbenzo[*lmn*][3,8]phenanthroline-1,3,6,8(2H,7H)-tetraone (**2**) (17.0 mmol, 1.00 eq) the solution turned red and was heated to reflux. The reaction mixture changed its color to green after 4 h and was cooled to room temperature. Quenching with 400 mL of ice water caused precipitation of a brown-grey solid, which was

filtered off and dried *in vacuo*. The solid was transferred into a soxhlet extractor and extracted with 1.50 L chloroform for one day. The extract was evaporated and recrystallized from 100 mL pyridine, yielding 3.10 g of a yellow solid (12.9 mmol, 76.0%).

^{1}H NMR (500 MHz, chloroform-d_1): δ 7.12 (s, 4H, *H*-Ar), 3.88 (s, 8H, CH_2), 2.57 ppm (s, 6H, CH_3); ^{13}C NMR (126 MHz, chloroform-d_1): δ 131.8 (C_q), 127,4 (C_q), 121.7 (CH), 58.7 (CH_2), 45.6 ppm (CH_3).

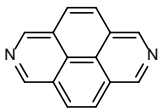

Benzo[*lmn*][3,8]phenanthroline[8] (DAP) (4): In a 250 mL flask equipped with a mechanical stirring bar, 7.70 g of selenium (97.3 mmol, 20.0 eq) and 1.20 g of 2,7-dimethyl-1,2,3,6,7,8-hexahydrobenzo[*lmn*][3,8]phenanthroline (**3**) (4.87 mmol, 1.00 eq) were stirred at 265°C for 4 h. The black viscous mixture was heated to 300°C for 1 h and then cooled to room temperature. 100 mL of 1 M aqueous HCl were added and stirred under reflux for 30 minutes. This procedure was repeated for three times in total and after each boiling the black solid was filtered off. The filtrates were combined and aqueous NaOH (5 M) was added until pH 12.0 was reached. The formed yellow precipitate was separated by filtration, dissolved in 1 M HCl, and precipitated again with 1 M NaOH. This procedure was repeated twice. The obtained precipitate was filtered off and dried *in vacuo*. The product was isolated as a yellow solid with a yield of 720 mg (3.52 mmol, 70.0%).

^{1}H NMR (500 MHz, chloroform-d_1): δ 9.48 (s, 4H, *H*-Ar), 8.17 ppm (s, 4H, *H*-Ar); ^{13}C NMR (126 MHz, chloroform-d_1): δ 145.5 (CH), 126.5 (C_q), 126.5 (C_q), 126.0 ppm (CH).

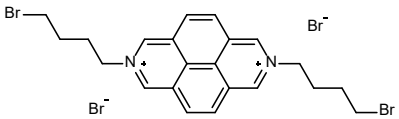

2,7-Bis(4-bromobutyl)benzo[*lmn*][3,8]phenanthroline-2,7-diium dibromide (5): A solution of 50.0 mg DAP (**4**) (245 µmol, 1.00 eq) was prepared in 10.0 mL dry DMF under nitrogen atmosphere. To the reaction solution 2.20 mL 1,4-dibromobutane (3.96 g, 18.4 mmol, 75.0 eq) were added and the reaction mixture was stirred at 75°C for 48 h. After cooling down, the yellow precipitate was filtered off, washed with copious amounts of DMF, and dried under reduced pressure. The isolated product was obtained as a yellow solid with a yield of 71.4 mg (112 µmol, 46.0%).

^{1}H NMR (500 MHz, D_2O): δ 10.11 (s, 4H, *H*-Ar), 8.85 (s, 4H, *H*-Ar), 5.23 (t, 4H, *J* = 7.5 Hz, CH_2), 3.56 (t, 4H, *J* = 6.4 Hz, CH_2), 2.54 (quin, 4H, *J* = 7.5 Hz, CH_2), 2.04 ppm (quin, 4H, *J* = 7.5 Hz, CH_2); ^{13}C NMR (126 MHz, D_2O): δ 141.1 (CH), 130.0 (C_q), 129.9 (CH), 127.0 (C_q), 63.9 (CH_2), 33.0 (CH_2), 30.1 (CH_2), 28.5 ppm (CH_2); HRMS (ESI) (pos., H_2O): m/z calcd. for $C_{22}H_{24}Br_2N_2^{2+}$: 238.0138 $[M]^{2+}$; found 238.0135.

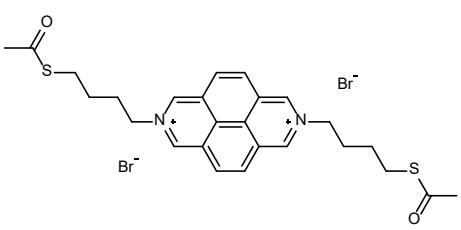

2,7-Bis(4-(acetylthio)butyl)benzo[*lmn*][3,8]phenanthroline-2,7-diium dibromide (6): In a vial, 113 mg of 2,7-bis(4-bromobutyl)-benzo[*lmn*][3,8]phenanthroline-2,7-diium dibromide (**5**) (178 µmol, 1.00 eq) were dissolved in 10.0 mL ultrapure water and 60.9 mg of potassium thioacetate (533 µmol, 3.00 eq) dissolved in 5.00 mL ultrapure water were added. The reaction solution was stirred for 2 days at room temperature under exclusion

of light. The solvent was removed under reduced pressure and the product was obtained as a brown solid with a yield of ≥99% due to remaining potassium thioacetate and used as such in the following synthetic step.
^{1}H NMR (500 MHz, D_2O): δ 10.10 (s, 4H, *H*-Ar), 8.85 (s, 4H, *H*-Ar), 5.21 (t, 4H, J = 7.4 Hz, C*H*$_2$), 2.96 (t, 4H, J = 7.4 Hz, C*H*$_2$), 2.35 (quin, 4H, J = 7.4 Hz, C*H*$_2$), 2.31 (s, 6H, C*H*$_3$), 1.75 ppm (quin, 4H, J = 7.4 Hz, C*H*$_2$); ^{13}C NMR (126 MHz, D_2O): δ 201.7 (C=O), 141.1 (CH), 130.0 (CH) 129.8 (C_q), 127.0 (C_q), 63.2 (CH_2), 30.2 (CH_2), 30.0 (CH_3), 27.8 (CH_2), 25.5 ppm (CH_2); HRMS (ESI) (pos., MeOH): m/z calcd. for $C_{26}H_{30}N_2O_2S_2^{2+}$: 233.0869 $[M]^{2+}$, found 233.0866.

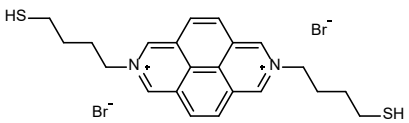

2,7-Bis(4-mercaptobutyl)benzo[*lmn*][3,8]phenanthroline-2,7-diium dibromide (7): 37.2 mg of 2,7-bis(4-(acetylthio)butyl)benzo[*lmn*][3,8]-phenanthroline-2,7-diium dibromide (**6**) (59.0 µmol, 1.00 eq) were dissolved in 5.00 mL dry MeOH and degassed with N_2 for 15 minutes. To the solution, 170 µL acetyl chloride (187 mg, 2.36 mmol, 40.0 eq) were added under nitrogen atmosphere and the mixture was stirred for 2.5 days at room temperature. The reaction mixture was quenched by the addition of water, causing the precipitation of a black solid. The solid was separated by filtration and the solvent was removed from the filtrate. The product was isolated as red-brown solid with a yield of 20.9 mg (38.4 µmol, 65.0%).
^{1}H NMR (500 MHz, D_2O): δ 10.10 (s, 4H, *H*-Ar), 8.86 (s, 4H, *H*-Ar), 5.21 (t, 4H, J = 7.4 Hz, C*H*$_2$), 2.63 (t, 4H, J = 7.0 Hz, C*H*$_2$), 2.40 (quin, 4H, J = 7.4 Hz, C*H*$_2$), 1.71 ppm (quin, 4H, J = 7.4 Hz, C*H*$_2$); ^{13}C NMR (126 MHz, D_2O): δ 141.1 (CH), 130.0 (CH), 129.8 (C_q), 127.0 (C_q), 63.3 (CH_2), 30.1 (CH_2), 29.5 (CH_2), 23.0 ppm (CH_2); HRMS (ESI) (pos., MeOH): m/z calcd. for $C_{22}H_{25}N_2S_2^+$: 381.1415 $[M-H]^+$, found 381.1450.

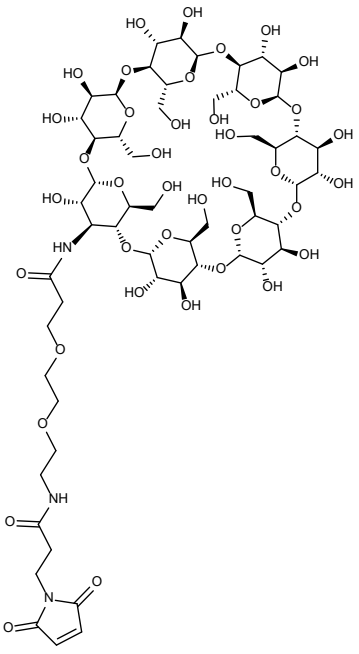

TEG-maleimide-β-CD (8): In a vial, 57.1 mg of 3A-amino-3A-deoxy-(2A*S*,3A*S*)-β-cyclodextrin hydrate (50.0 µmol, 1.00 eq) and 23.8 mg of maleimide-PEG$_2$-NHS ester (56.0 µmol, 1.20 eq) were combined and dried *in vacuo* to remove water from the solids as maleimides are sensitive to hydrolysis. The solids were dissolved in 10 mL dry DMF and the mixture was degassed with nitrogen. After the addition of 100 µL of NEt_3 (721 µmol, 14.4 eq) the reaction solution was stirred overnight at room temperature. The solvent was removed under reduced pressure and the residue was dissolved in 2.00 mL deionized water and purified by HPLC (gradient: 0-100 % ACN in water, 0.1% TFA). The product was isolated as a colorless powder with a yield of 61.8 mg (48.5 µmol, 85.0%).
^{1}H NMR (500 MHz, D_2O): δ 6.88 (s, 2H, C*H*), 5.08-4.99 (m, 6H, C*H*), 4.94 (d, 1H, J = 5.8 Hz, C*H*), 4.27 (s (br), 1H, C*H*), 3.95-3.53 (m, 52H, C*H*, C*H*$_2$), 3.34-3.32 (m, 2H, C*H*$_2$), 2.60-2.51 ppm (m, 4H, C*H*, C*H*$_2$); HRMS (ESI) (pos., MeOH): m/z calcd. for $C_{56}H_{89}N_3O_{40}H^+$: 1444.5095 $[M+H]^+$, found 1444.5083.

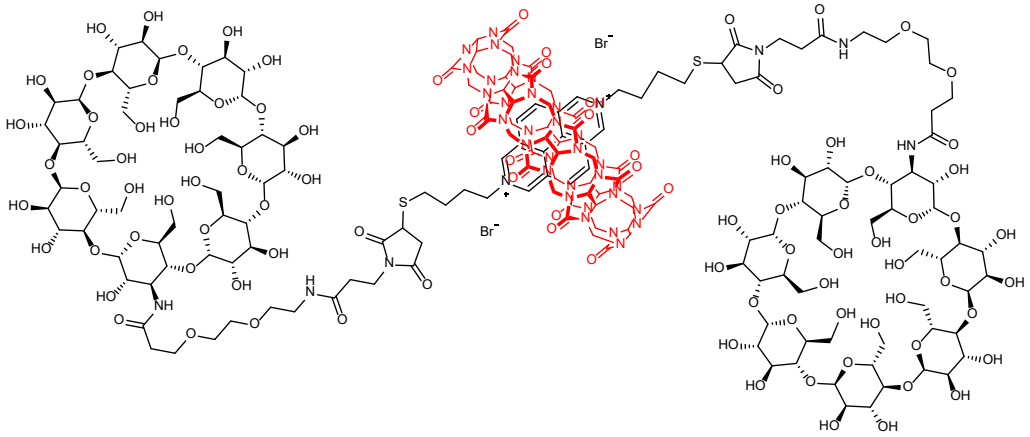

Rotaxane (1): In a vial, 50.0 mg cucurbit[8]uril (38.0 µmol, 1.10 eq) were dissolved in 50 mL ultrapure water and 14.5 mL of a 2.4 mM aqueous solution of 2,7-bis(4-mercaptobutyl)benzo[*lmn*][3,8]phenanthroline-2,7-diium dibromide (**7**) (18.9 mg, 35.0 µmol, 1.00 eq) were added to the solution. Before synthesis, the thiol concentration (2 equiv. per dye molecule) of **7** was determined through the Ellman test.[9] The mixture was diluted with 8.00 mL of sodium phosphate buffer, pH 7.7, causing a color change from yellow to bright green. After sonication for 15 minutes, 111 mg TEG-maleimide-β-CD (**8**) (77.0 µmol, 2.20 eq) were added and the mixture was stirred at room temperature overnight, resulting in a slow color change from green back to yellow. The solvent was removed under reduced pressure and the residue was washed with 1:1 EtOH:water three times, with subsequent removal of white solid by centrifugation. The combined solutions were dried *in vacuo* and purification was done by HPLC (mobile phase: 17% ACN in water (0.1% TFA) for 45 minutes then 100% ACN for 15 minutes). The product was obtained as a yellow solid with a yield of 59.4 mg (12.4 µmol, 35.0%). The product formation was confirmed by ^{1}H NMR, see also main text Fig. 2.

HRMS (ESI) (pos., 1:1 ACN/H_2O, 1% formic acid): m/z calcd. for $C_{182}H_{252}N_{40}O_{96}S_2^{2+}$: 2299.2765 $[M]^{2+}$; found 2299.7039.

c. Additional synthetic routes that led to poorly water-soluble rotaxanes

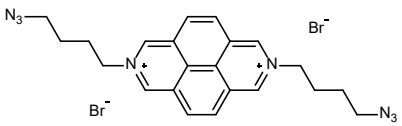

2,7-Bis(4-azidobutyl)benzo[*lmn*][3,8]phenanthroline-2,7-diium dibromide (9): A solution of 25.0 mg of 2,7-bis(4-bromobutyl)benzo[*lmn*][3,8]phenanthroline-2,7-diium dibromide (**5**) (39.4 µmol, 1.00 eq) was prepared in 2.5 mL deionized water and mixed with a solution of sodium azide (17.1 mg, 262 µmol, 6.60 eq) pre-dissolved in 2.5 mL ultrapure water. The reaction mixture was heated up to 80°C for 3 h before it was concentrated *in vacuo*. The product was isolated as a yellow solid with a yield of 19.1 mg (34.1 µmol, 87.0%).

^{1}H NMR (500 MHz, D_2O): δ 10.12 (s, 4H, *H*-Ar), 8.86 (s, 4H, *H*-Ar), 5.24 (t, 4H, J = 7.4 Hz, C*H*$_2$), 3.45 (t, 4H, J = 6.6 Hz, C*H*$_2$), 2.38 (quin, 4H, J = 7.4 Hz, C*H*$_2$), 1.77 ppm (quin, 4H, J = 7.4 Hz, C*H*$_2$); ^{13}C NMR (126 MHz, D_2O): δ 141.1 (CH), 130.0 (C_q), 129.8 (C_q), 127.0 (C_q), 63.3 (CH_2), 50.3 (CH_2), 28.8 (CH_2), 25.0 ppm (CH_2).

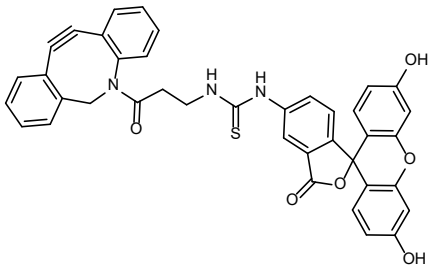

DBCO-fluorescein[10] (10): 14.8 mg of 5-isothiocyanate fluorescein (39.0 µmol, 1.10 eq) and 9.8 mg of DBCO-amine (35.0 µmol, 1.00 eq) were dissolved in a mixture of acetonitrile and carbonate puffer, pH 10.0 (v:v 3:1). The mixture was stirred for 7 days at room temperature and the reaction progress was controlled via TLC (ethyl acetate as mobile phase, colored with Seebach solution). The reaction solvent was removed under reduced pressure. The crude product was used without further purification and therefore no NMR spectra suitable for characterization was recorded.

HRMS (ESI) (pos., MeOH): m/z calcd. for $C_{39}H_{27}N_3O_6SNa^+$: 688.1513 $[M+Na]^+$, found 688.1604.

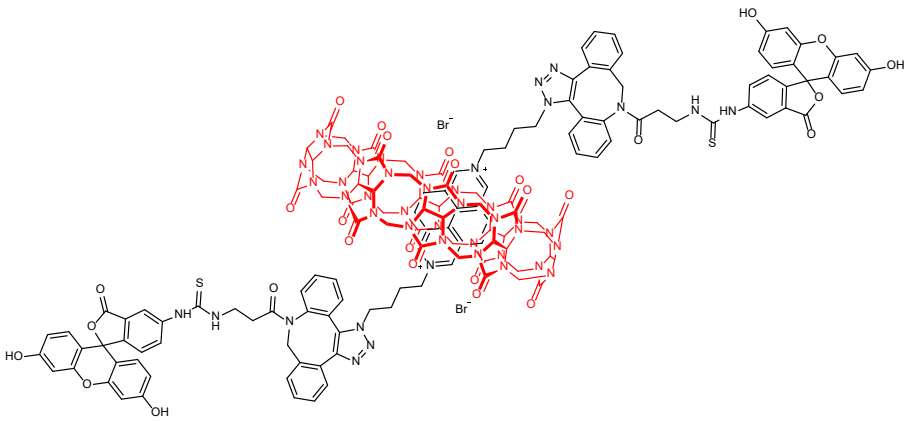

DBCO-fluorescein rotaxane (11): In a reaction flask, 3.60 mg of 2,7-Bis(4-azidobutyl)benzo[*lmn*][3,8]-phenanthroline-2,7-diium dibromide (**9**) (9.00 µmol, 1.00 eq) were dissolved in ultrapure water and 14.3 mg of CB8 (10.8 µmol, 1.20 eq) were added as solid. The reaction mixture was stirred for 30 minutes at room temperature. Subsequently, 18.0 mg of DBCO-fluorescein (**10**) were added and the reaction mixture was stirred for 4 days at room temperature. A red precipitate was formed and filtered off. The remaining reaction solution was overlaid with 7.5 mL methanol and stored in the fridge for 1 day. The formed precipitate was filtered off and combined with the previously gained red solid. NMR analysis was not possible due to low solubility of the product.

HRMS (ESI) (neg., DMSO/H_2O 1:1): m/z calcd. for $C_{148}H_{126}N_{46}O_{28}S_2^{2+}$: 1529.8493 $[M]^{2+}$, found 1529.9763.

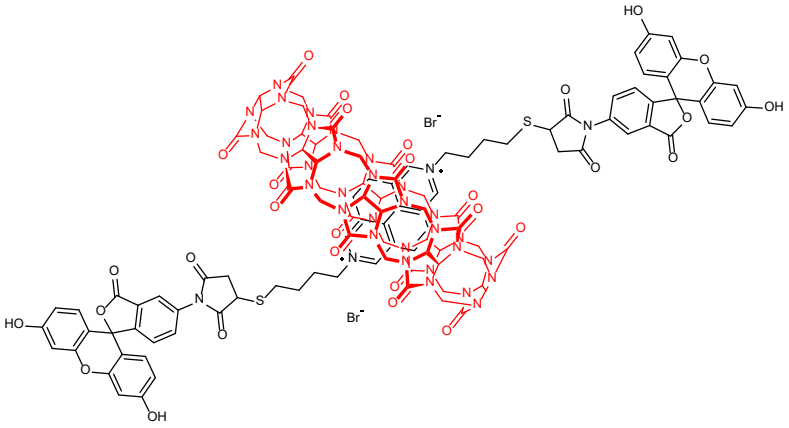

FITC-rotaxane (12): 949 µg of 2,7-bis(4-(acetylthio)butyl)benzo[*lmn*][3,8]phenanthroline-2,7-diium dibromide (**7**) (1.75 µmol, 1.00 eq) were dissolved in ultrapure water and 3.50 mg of CB8 (2.63 µmol, 1.50 eq) were added as solid. The reaction mixture was stirred at room temperature for 30 minutes. Fluorescein-5-maleimide was dissolved in dry DMSO with a final concentration of 1 mM. 3500 µL (equal to 1.50 mg, 3.5 µmol, 2.00 eq) of this 1 mM solution were added to the aqueous reaction mixture, which was stirred for 3 days. The reaction mixture was dried *in vacuo*, redissolved in water and lyophilized. Several purification attempts such as normal phase column chromatography and crystallization failed. HPLC purification was proceeded by running a gradient from 20% ACN to 60% ACN in water containing 0.1% TFA. NMR analysis was not possible due to low solubility of the product.

HRMS (ESI) (pos., DMSO/H_2O 3:1): m/z calcd. for $C_{118}H_{110}N_{36}O_{30}S_2$: 1282.8432 $[M]^{2+}$, found 1282.7911.

d. Characterization of rotaxane 1 (DOSY and DLS)

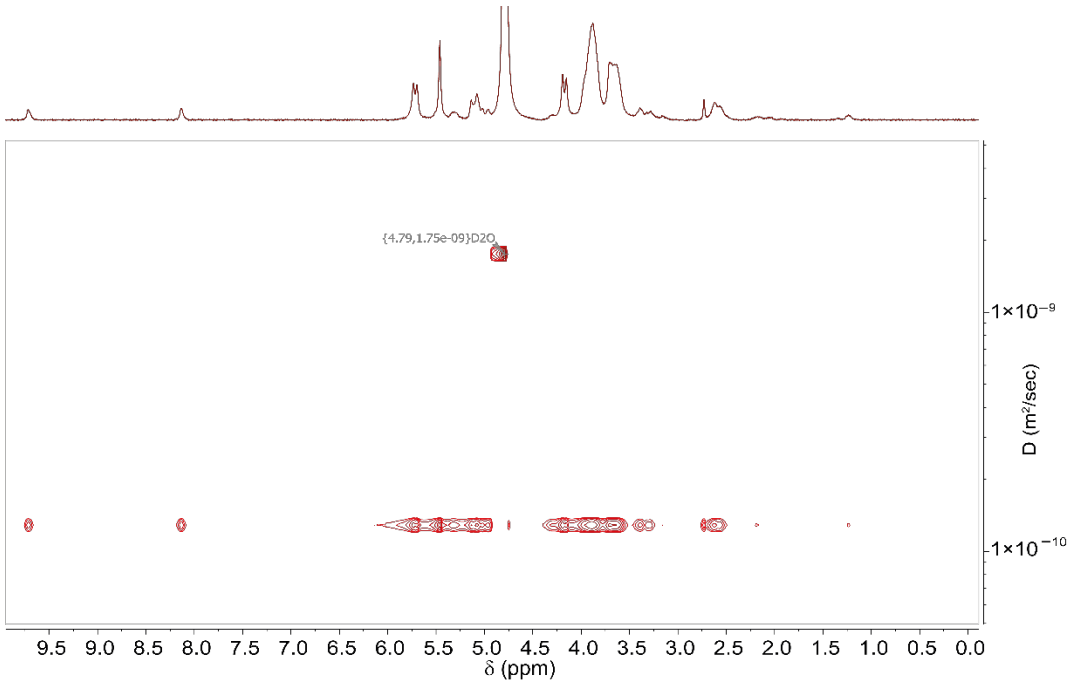

Supplementary Fig. 1. ^{1}H NMR of rotaxane **1** with marked signal peaks and the corresponding 2D DOSY spectrum measured in D_2O.

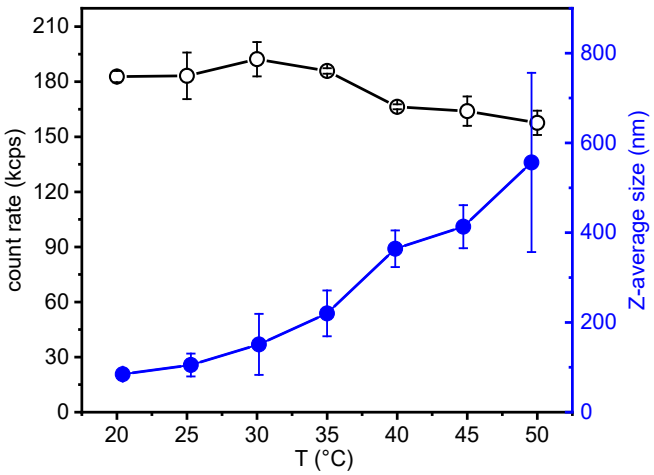

Supplementary Fig. 2. Temperature dependent count rates (black) and the Z-average size (blue) of rotaxane **1** within a temperature range from 20 to 50°C. An increase of the Z-average size with rising temperature indicates the formation of large aggregates, which is a known behaviour of cyclodextrins.[11]

2. Fluorescence titration experiments and binding isotherms

The analyte-sensing functionality of rotaxane **1** as chemosensor was tested by an emission-based analyte assay with indole (see Supplementary Fig. 3). The response of rotaxane **1** towards indole remained similarly strong in 1X PBS as in water while the bimolecular chemosensor CB8•MDAP almost loses its functionality in PBS due to its salt-binding induced disassembly (weaker emission quenching compared to rotaxane **1** observed). The addition of the competitively CB8 binding 1-adamantanol (AdOH) further verified the superiority of rotaxane **1** over the non-interlocked analogue CB8•dye chemosensor: Rotaxane **1** is unaffected by the presence of AdOH whereas both the MDAP dye and the analyte indole are displaced from CB8 in the presence of AdOH causing a strong fluorescence increase.

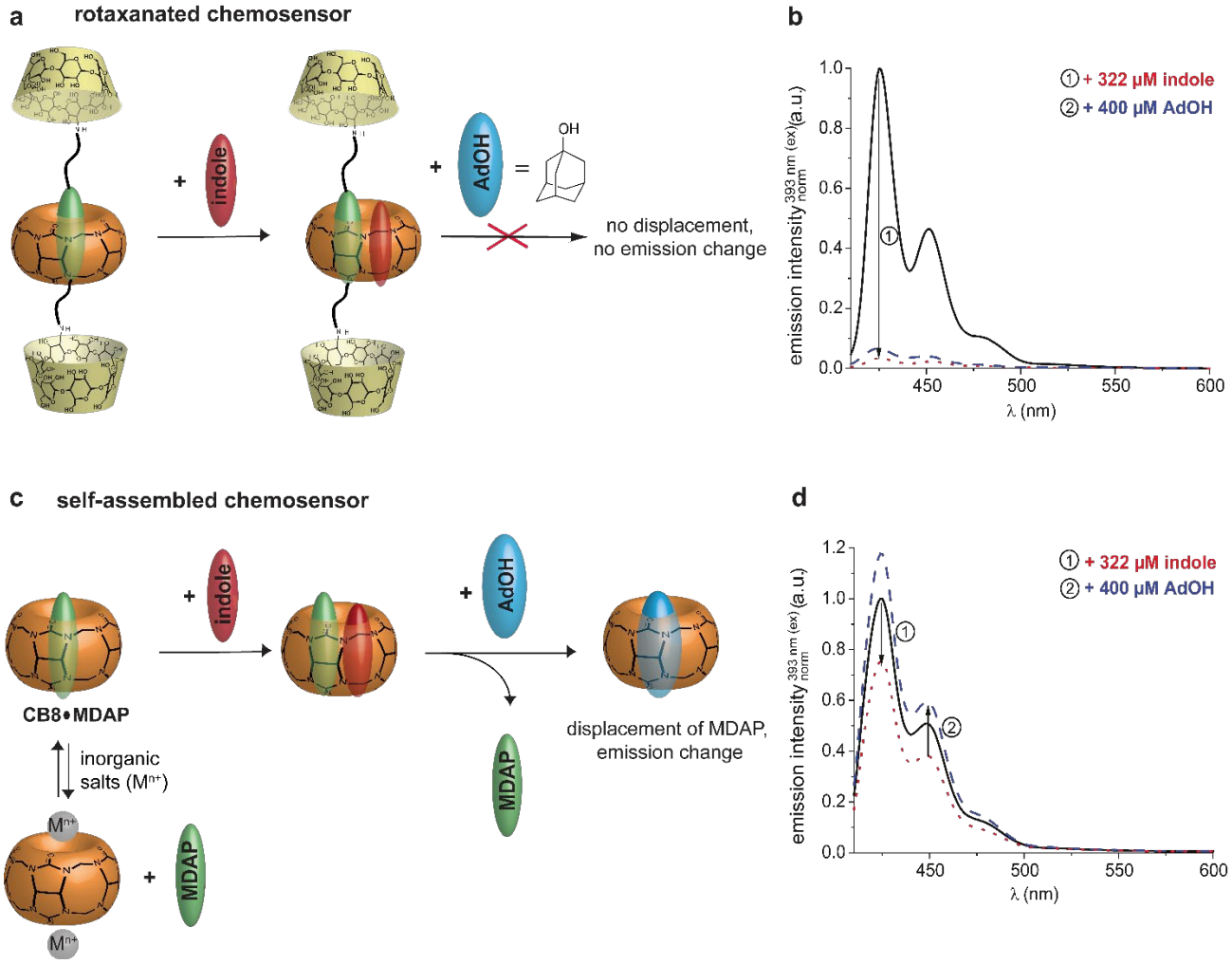

Supplementary Fig. 3. a Schematic representation of the analyte binding of rotaxane **1** for the electron-rich aromatic analyte indole and for the bulky (not size-fitting) analyte 1-adamantanol. **b** Emission quenching is observed after addition of indole due to the dye-analyte interaction whereas the presence of 1-adamantanol does not cause any signal change. **c** Schematic representation of analyte binding to a self-assembled CB8•MDAP chemosensor. Bulky and strongly binding analytes such as 1-adamantanol displace the bound dye and thereby disassemble the chemosensor. **d** Emission response of the CB8•MDAP chemosensor to the presence of indole and adamantanol. The higher emission signal compared to the starting signal after adamantanol addition indicates the disassembly. All emission spectra were recorded in 1X PBS (black) at 25°C (λ_{ex} = 393 nm).

Binding affinity determination in a direct binding assay (DBA)

$$\text{rotaxane} + G \rightleftharpoons \text{rotaxane} \bullet G$$

$$K_a^{\text{rotaxane} \bullet G} = \frac{[\text{rotaxane} \bullet G]}{[\text{rotaxane}]\,[G]}$$

$$[\text{rotaxane}]_0 = [\text{rotaxane} \bullet G] + [\text{rotaxane}]$$

$$[G]_0 = [\text{rotaxane} \bullet G] + [G]$$

$$I = I_0 + I_{\text{rotaxane} \bullet G} \times [\text{rotaxane} \bullet G] + [G] + I_G \times [G]$$

with K_a = binding constant, G = guest/analyte, I = emission intensity

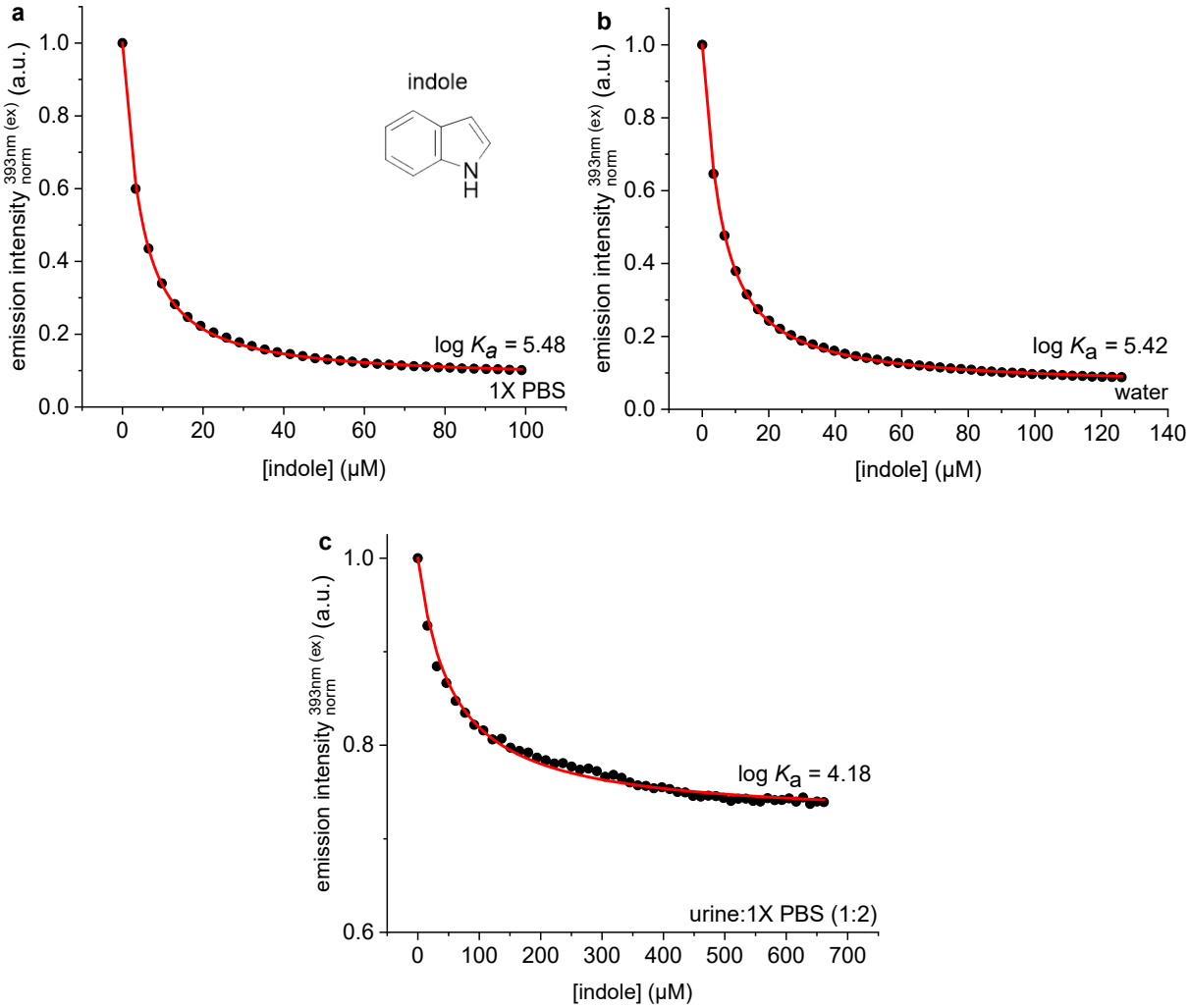

Supplementary Fig. 4. Representative DBA binding isotherms determined by emission-based titration measurements (λ_{ex} = 393 nm, λ_{em} = 450 nm) of **a** indole (0 - 100 μM) to rotaxane **1** (2.5 μM) in 1X PBS at 25°C, **b** indole (0 - 126 μM) to rotaxane **1** (2.5 μM) in water at 25°C, and **c** indole (0 - 663 μM) to rotaxane **1** (1.0 μM) in urine (1:2 in 1X PBS) at 25°C. Acquired data is depicted by black dots. The fit according to a 1:1 binding model is shown as a red line.

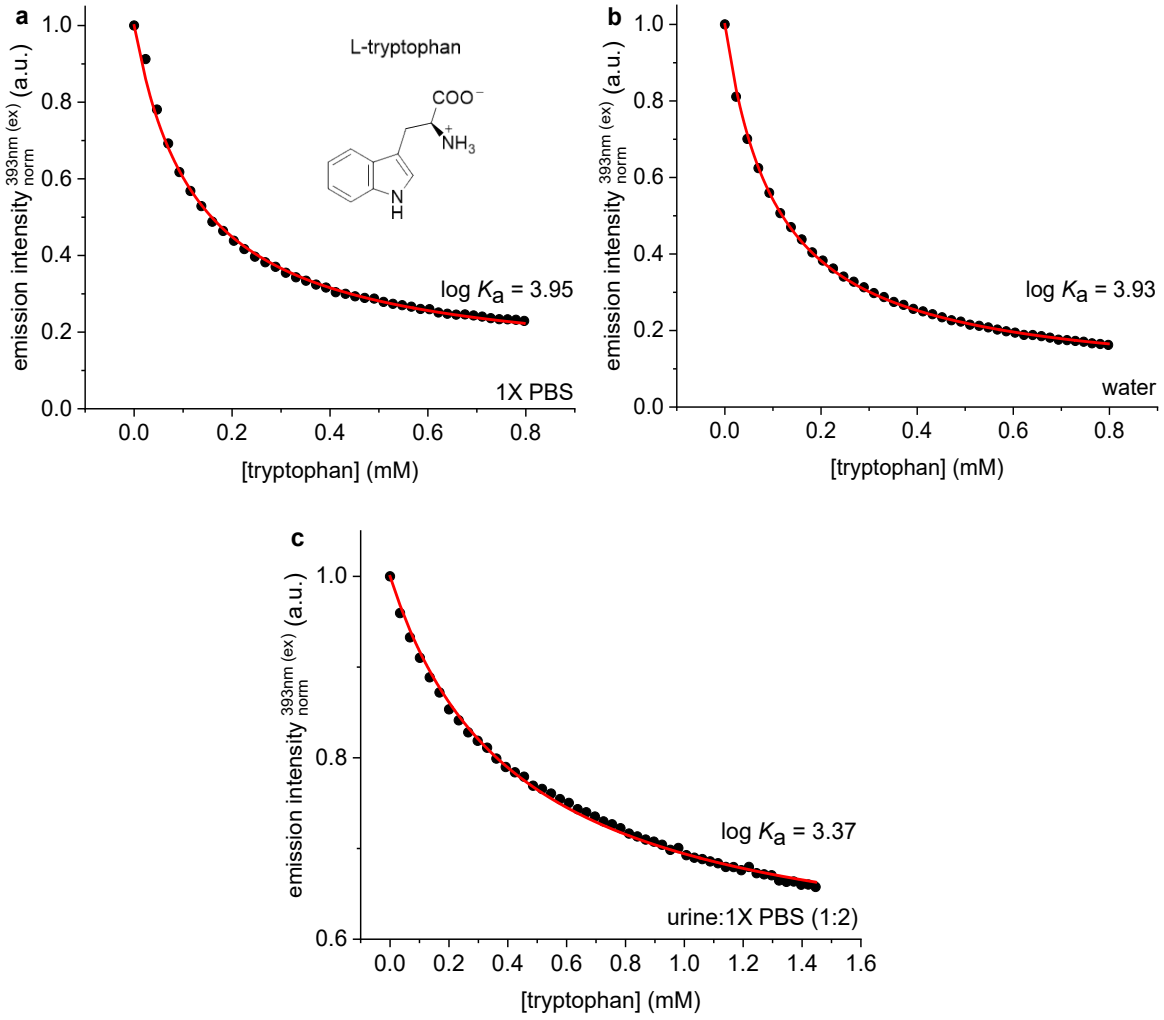

Supplementary Fig. 5. Representative DBA binding isotherms determined by emission-based titration measurements (λ_{ex} = 393 nm, λ_{em} = 450 nm) of **a** tryptophan (0 - 797 µM) to rotaxane **1** (2.5 µM) in 1X PBS at 25°C, **b** tryptophan (0 - 797 µM) to rotaxane **1** (2.5 µM) in water at 25°C, and **c** tryptophan (0 - 1.44 mM) to rotaxane **1** (1.0 µM) in urine (1:2 in 1X PBS) at 25°C. Acquired data is depicted by black dots. The fit according to a 1:1 binding model is shown as a red line.

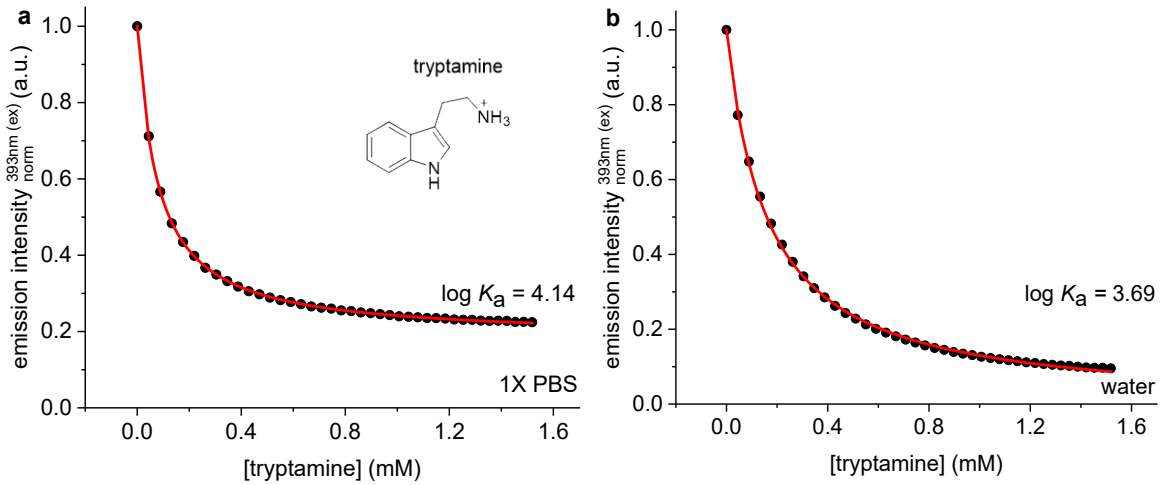

Supplementary Fig. 6. Representative DBA binding isotherms determined by emission-based titration measurements (λ_{ex} = 393 nm, λ_{em} = 450 nm) of **a** tryptamine (0 - 1.5 mM) to rotaxane **1** (2.5 µM) in 1X PBS at 25°C and **b** tryptamine (0 - 1.5 mM) to rotaxane **1** (2.5 µM) in water at 25°C. Acquired data is depicted by black dots. The fit according to a 1:1 binding model is shown as a red line.

The emission response of rotaxane **1** upon addition of aliquots of bioorganic analytes was determined in a plate reader format at 450 nm (λ_{ex} = 393 nm). Specifically, microwells were equipped with 100 µl of 3.0 µM rotaxane **1** in 1X PBS each. Subsequently, the analyte stock solutions were added to the wells and diluted with 1X PBS buffer to reach a final volume of 300 µL to give a concentration of 1.0 µM for rotaxane **1**, and 100 µM, 500 µM, and 1.0 mM of each analyte. 1X PBS was used for blank correction and the emission intensity of a 1.0 µM solution of rotaxane **1** was used as reference. All measured emission intensities were averaged over the repetitions performed (≥4) and blank corrected. The emission quenching values were then calculated according to

$$\text{emission quenching} = \frac{I_{(\text{rotaxane})} - I_{(\text{rotaxane+analyte})}}{I_{(\text{rotaxane})}}$$

with $I_{(\text{rotaxane + analyte})}$ and $I_{(\text{rotaxane})}$ as emission intensity of rotaxane **1** (1.0 µM) in the presence and absence of the analyte, respectively. The obtained data are shown as bar graphs in Fig. 3d in the main part.

3. Analyte assays in real serum samples

a. HPLC-based quantification of L-Trp in serum samples

The quantification of the L-tryptophan concentration of three different blood serum samples was done using common HPLC methods according to literature.[12]

Calibration curve: A calibration curve with five different L-Trp concentrations (final concentrations: 5, 20, 40, 60, and 80 µM) was obtained with a standard stock solution of 4.9 mM of L-tryptophan in 312 mM perchloric acid. Each concentration of L-tryptophan was determined through at least two measurements using a mobile phase of 10% acetonitrile in water with a flow rate of 1.2 mL/min and an injection volume of 20 µL. The calibration curve was obtained by plotting the integrated peak area of the fluorescence signal (λ_{ex} = 285 nm, λ_{em} = 353 nm) versus the standard concentrations. The slope and regression parameters were calculated by linear regression.

Unknown serum samples: The three serum samples with unknown Trp concentration were deproteinized by adding an equal volume (6 mL) of 624 mM of perchloric acid solution to 6 mL of the serum followed by careful mixing. The samples were stored on ice for 10 min for full precipitation and centrifuged at 10 000 rpm at +4°C for 10 min. Subsequently, the supernatant was separated from the protein and 20 µL of the supernatant were injected into the HPLC system for analysis. The obtained peaks of each serum were used to for the concentration determination of L-Trp by integrating the peak area of the fluorescence signal (λ_{ex} = 285 nm, λ_{em} = 353 nm) according to the following equation (Note: factor 2 used as samples are 1:1 diluted with perchloric acid):

$$\text{Trp in serum } (\mu M) = \frac{(\text{peak area of Trp in serum sample})}{(\text{peak area of Trp in standard solution})} \text{ x } 2$$

For each serum sample at least two measurements were done, and the integrated peak areas were averaged. Besides the determination of the native L-tryptophan serum concentration, each serum was additionally spiked with 25 µM of L-Trp (in 312 mM perchloric acid) to mimic abnormal high Trp levels and 20 µL were injected into the HPLC system for analysis. The determined L-Trp concentrations of each serum are shown in Supplementary Table 2.

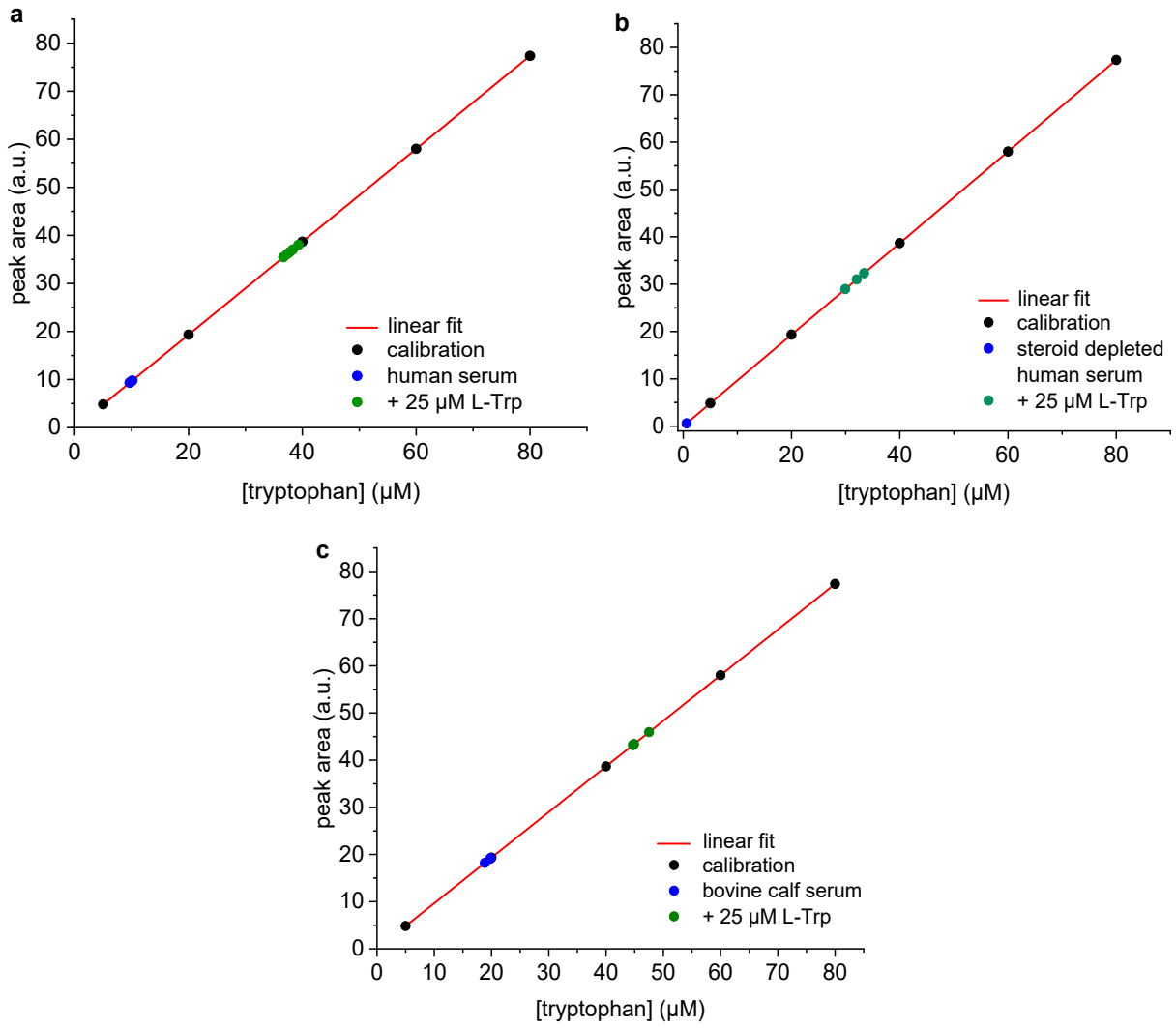

Supplementary Fig. 7. Plots of the linear calibration curve (black dots and red line) and the integrated peak area of the fluorescence signal (λ_{ex} = 285 nm, λ_{em} = 353 nm) of the serum samples (blue) and tryptophan-spiked serum samples (green). **a** Human serum measured in 4 replica measurements, **b** steroid depleted human serum measured in 3 replica measurements, and **c** bovine calf serum measured in 3 replica measurements. All replicas are shown as individual data points.

b. Rotaxane assay for L-Trp determination in non-deproteinized blood serum samples

The emission quenching (EQ) of rotaxane **1** in the presence of three different blood serum samples was determined by utilizing rotaxane **1** at a concentration of 10 µM in a plate reader format at 450 nm (λ_{ex} = 393 nm). Blood serum samples were used as such without deproteinization (further called 'untreated'). For each serum sample, at least 8 repetitions were conducted, which were used to obtain an averaged value for each measurement step. Accordingly, for each run the wells of a 96 well plate were equipped with 250 µL of one of the serum samples. Then, 5.1 µL of a 100 µM rotaxane **1** stock solution were added to every well to reach a concentration of 10 µM for rotaxane **1.** After mixing, the emission intensity was obtained (I_1). Subsequently, 5.2 µL of a 1.25 mM L-tryptophan stock solution were added to all wells to reach a L-Trp concentra-

tion of 25 µM and the emission intensity was obtained after mixing (I_2) for each serum sample. Finally, the full emission quenching (I_3) of rotaxane **1** was achieved by adding 10 µL of a 4.3 mM indole stock solution to reach a final indole concentration of 160 µM in each well. The autofluorescence (I_0) of each of the serum samples was measured as control. Errors were generously estimated based on our former experiments with plate reader measurements setups. For the measurements with rotaxane **1** in blood serum, the observed errors were much smaller than the generously estimated error ranges.

The obtained emission intensity was normalized by division with the emission intensity of 10 µM rotaxane **1** solution in water (I_{ref}). The normalized EQ for each serum sample and the spiked serum samples was determined according to the following equations using the full emission quenching of rotaxane **1** with indole (I_3) and the emission intensity of rotaxane **1** in water (I_{ref}) as reference:

$$\mathrm{EQ(serum)} = \frac{I_1 - I_{ref}}{I_3 - I_{ref}} \qquad \mathrm{EQ(spiked\ serum)} = \frac{I_2 - I_{ref}}{I_3 - I_{ref}}$$

with I_1 = emission intensity of rotaxane **1** in serum

I_2 = emission intensity of rotaxane **1** in spiked serum (+25 µM Trp)

I_3 = emission intensity of rotaxane **1** in serum after indole addition

I_{ref} = emission intensity of rotaxane **1** in water

The corresponding emission quenching of each blood serum sample as well as their L-tryptophan spiked serum samples are shown in a bar graph in Fig. 4 in the main text.

4. Monitoring of label-free enzymatic reactions in real time

The enzymatic digestion of the protein bovine serum albumin (BSA) by pepsin was monitored through intensity changes of the rotaxane **1** emission in real time. BSA cannot bind to the rotaxane **1** due to its compact structure in which hydrophobic amino acids such as Phe and Trp are buried inside the protein core. The endopeptidase pepsin breaks the protein down into smaller peptides carrying exposed amino acids on their surface, which can be bound and thus detected by the rotaxane chemosensor.

Stock solutions of BSA and rotaxane **1**, both in 1X PBS at pH 2.0, were mixed to reach a final concentration of 100 µg/mL BSA and 4.5 µM of **1**. After equilibration (~100 s), the emission intensity was monitored (λ_{ex} = 393 nm, λ_{em} = 450 nm) over time. Different volumes of a pepsin stock solution (in 1X PBS, pH 2.0) were added to reach pepsin concentrations in a range of 0 - 70 µg/mL in the cuvette and the fluorescence kinetic traces were monitored for 20 min. As control experiments, the time course of a BSA-rotaxane mixture without pepsin addition and pepsin addition to rotaxane **1** in the absence of BSA were recorded.

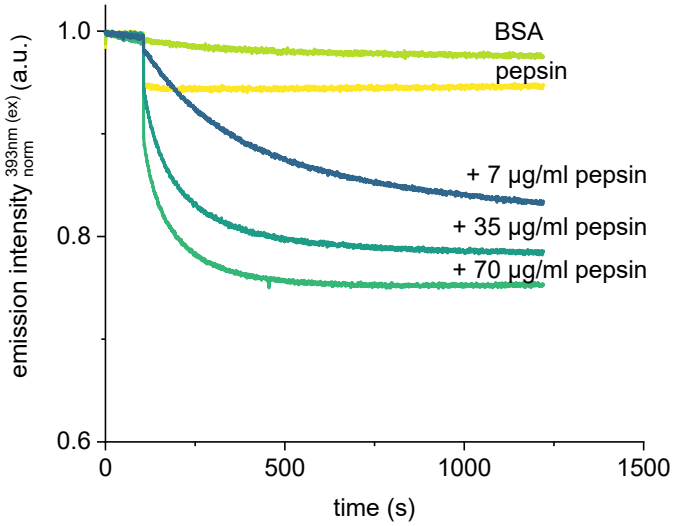

Supplementary Fig. 8. Fluorescence kinetic traces for the enzymatic hydrolysis of 100 µg/mL BSA in the presence of rotaxane **1** (4.5 µM) by pepsin (0 - 70 µg/mL) monitored at 450 nm (λ_{ex} = 393 nm) in 1X PBS (pH 2.0) at 25°C. The expected faster hydrolysis of BSA with increasing pepsin concentration was observed.

5. Structured immobilization by microcontact printing of rotaxane 1

The immobilization of rotaxane **1** was conducted using microchannel cantilever spotting (µCS). For a detailed description of the experimental setup see methods section in main part. The sensitivity of the rotaxane **1** microarrays for analyte detection was examined by the incubation with solutions of L-tryptophan at different concentrations. The mean emission intensities of the spots of the microarrays before and after the incubation with the corresponding analyte and the corresponding fluorescence images are shown in Supplementary Fig. 9. It is possible to detect tryptophan concentrations down to 10^{-8} M which is indicated by the greater emission decrease of the rotaxane **1** microarray after the incubation with 10^{-8} M compared to the control with 1X PBS. However, a concentration of 10^{-9} M of L-tryptophan seems to be no longer discernible from pure PBS.

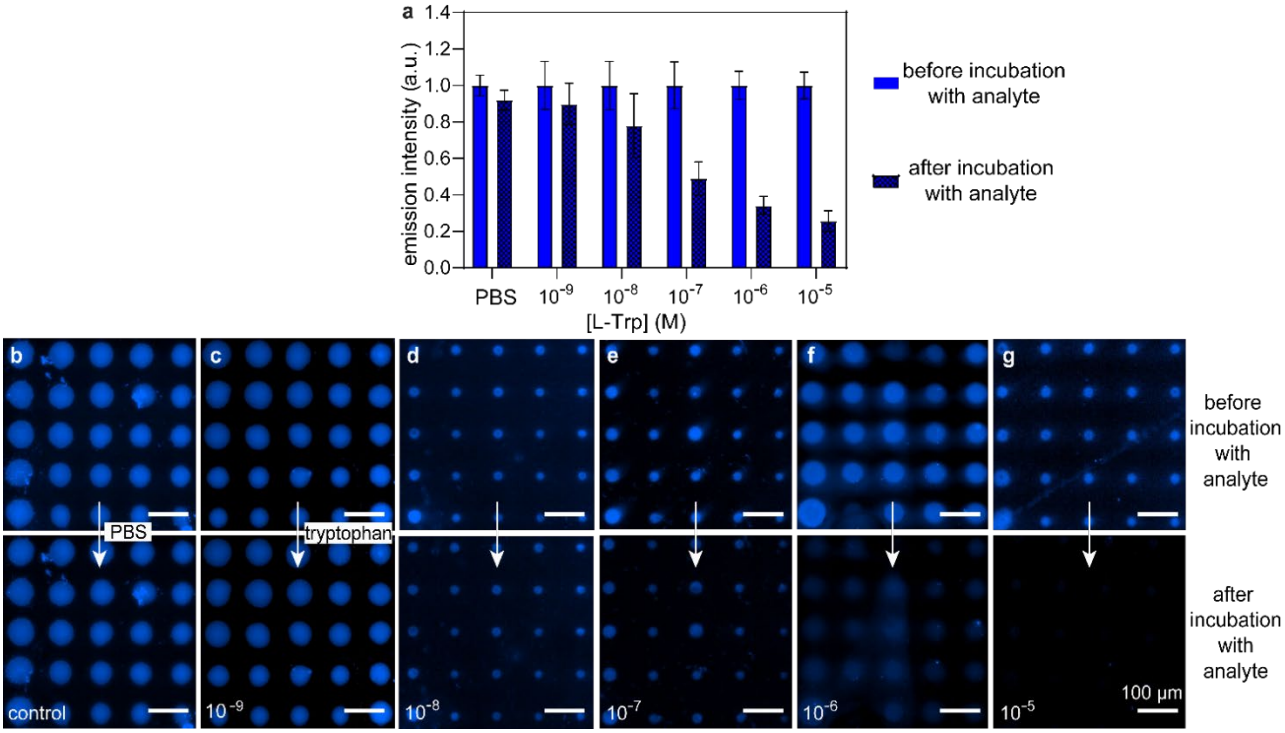

Supplementary Fig. 9. Tryptophan detection at different concentrations on rotaxane **1** microarrays. **a** Quantification of the mean fluorescence intensities of the rotaxane **1** microarray spots before and after the incubation with tryptophan solutions of different concentrations and with PBS as control. **b-g** Fluorescence images of the rotaxane **1** microarrays before and after the incubation with tryptophan solutions of various concentrations. Images were taken with 10 s exposure time and a DAPI filter. Scale bars equal to 100 µm. See also Supplementary Table 3.

As control experiments, a CB8•MDAP chemosensor microarray was set up according to previous work.[13] CB8 ink containing 1 mg/mL of propargyl-functionalized CB8 (in DMSO containing 40% TCEP dissolved in water (3 mg/mL) and 20% glycerol) was micropatterned on thiol surfaces (SiO_2–SH) via µCS to obtain the CB8 microarray. After printing, the substrate was irradiated with UV light (254 nm) for 10 min, then washed with water and ethanol, and finally dried by a N_2 stream. The remaining free thiols of the surface were blocked through incubation with an aqueous *N*-ethylmaleimide (10mg/mL, blocking agent) solution at pH 7.0 for 2 h. Then, the substrate was covered with 20 µL of a 50 µM MDAP solution for 1 min, then washed with water and dried with a N_2 stream to obtain the CB8•MDAP chemosensor array.

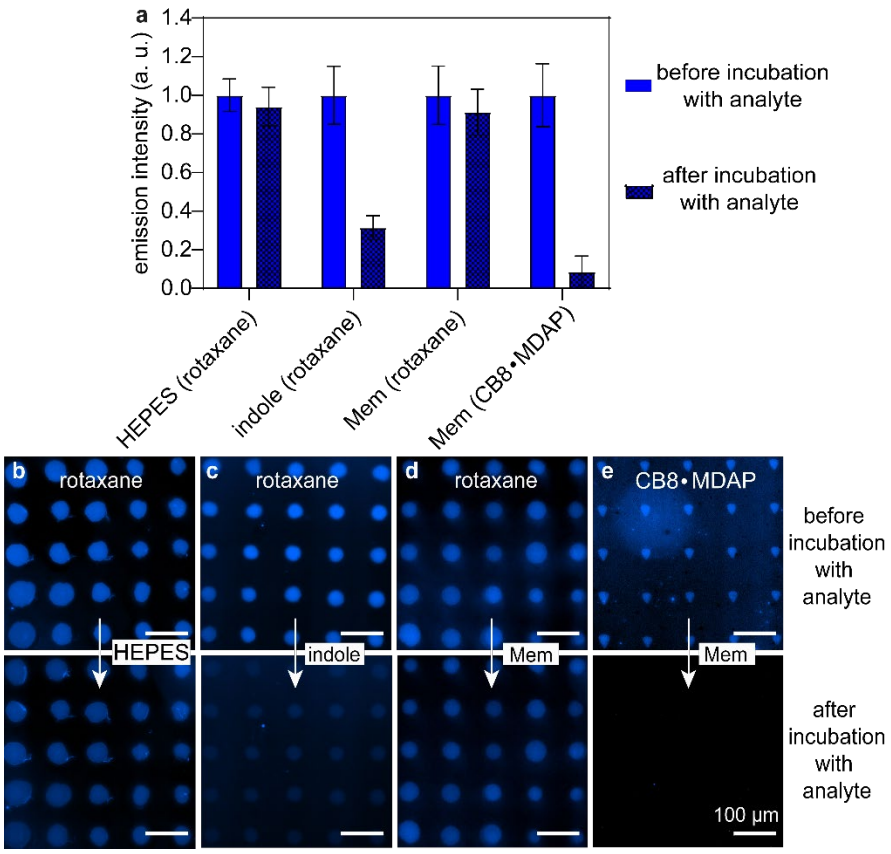

Supplementary Fig. 10. Detection of different analytes with rotaxane **1** and CB8•MDAP microarrays. **a** Quantification of the mean fluorescence intensities of the microarray spots before and after the incubation with different analytes. **b-e** Fluorescence images of the microarrays before and after incubation with an analyte (10 µM) or pure HEPES as control. Images were taken with 10 s exposure time and DAPI filter. Scale bars equal 100 µm. See also Supplementary Table 4.

The response of the CB8•MDAP microarray towards the presence of an analyte is shown in Supplementary Fig. 10. in comparison to the response of rotaxane **1** microarrays with different analytes in HEPES buffer. The incubation of the rotaxane **1** array with pure HEPES buffer as a negative control shows no significant decrease in fluorescence. As expected, the emission intensity of rotaxane **1** decreased for the incubation with indole showing that indole binds to the immobilized rotaxane **1** and thereby quenches the emission of the DAP dye. In contrast, the incubation of the rotaxane **1** microarray with memantine, an analyte that has a higher binding affinity towards CB8 than DAP, shows only an insignificant emission change, indicating that the analyte is not bound. In contrast, the CB8•MDAP microarray shows an almost 100% emission quenching upon incubation with memantine, indicating that the MDAP dye is displaced by the bigger and stronger binding analyte memantine.[13]

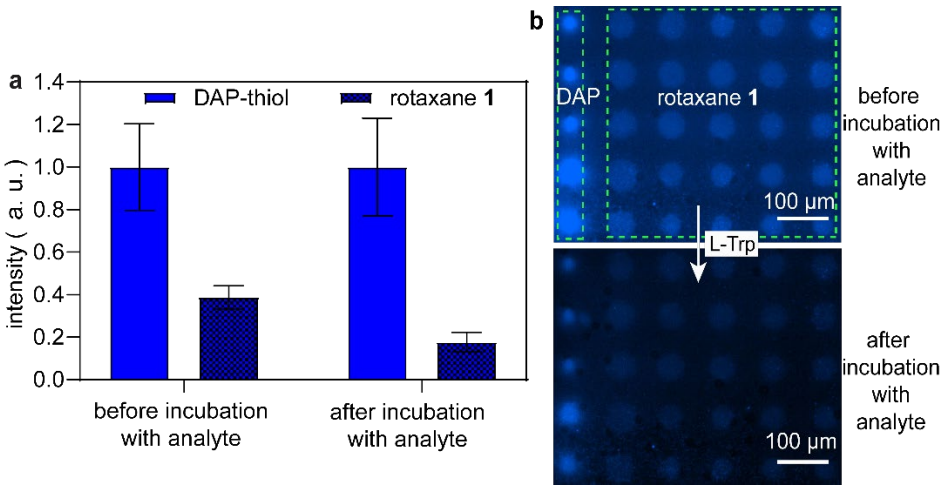

Supplementary Fig. 11. Tryptophan detection by ratiometric rotaxane **1** microarrays with surface-bound DAP dye as reference dye. **a** Quantification of the mean fluorescence intensities of the microarray spots before and after incubation with tryptophan solution (10 µM in 10 mM HEPES buffer). **b** Fluorescence images of the ratiometric rotaxane **1** microarray before and after incubation. Images were taken with 10 s exposure time, DAPI filter. Scale bars equal 100 µm. See also Supplementary Table 5.

In a ratiometric rotaxane **1** microarray a column of DAP-thiol molecules (without CB8) was printed beside the microarray as a reference (Supplementary Fig. 11). After tryptophan incubation, the fluorescence intensity of the rotaxane **1** spots was quenched compared to the DAP spots, in accordance with the expected binding of tryptophan to the rotaxane **1**, and thereby excluding the hypothetical dynamic quenching of the DAP fluorophore by Trp.

6. Representative synthetic binders for Trp

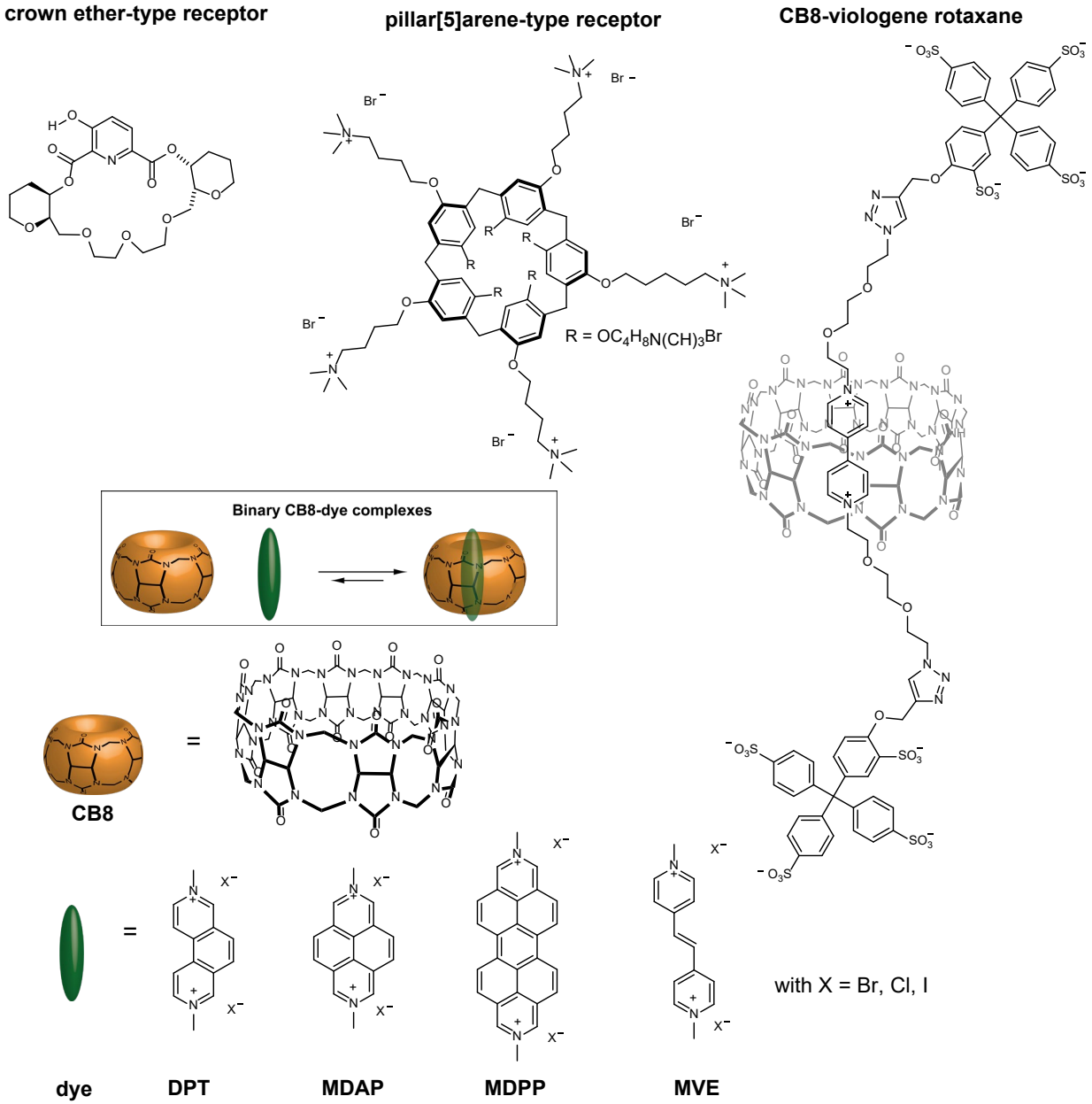

Supplementary Fig. 12. Chemical structures of representative synthetic binders for tryptophan. See also Table 2 in the main text.

7. Supplementary Tables

Supplementary Table 1. Typical L-tryptophan concentration ranges for healthy and diseased adults in blood serum, blood plasma, and urine.

	concentration (µM)	medium	ref.
no disease	53 - 77	blood serum	[14]
	21 - 93	urine	[15]
Alzheimer's disease	24 - 42	blood serum	[16]
	15 - 22	urine	[16]
chronic kidney disease	17 - 26	blood serum	[12]
cardiovascular disease	27 - 76	blood serum	[17]
anemia of inflammation	22 - 43	blood serum	[18]
coronary heart disease	44 - 63	blood plasma	[19]
sepsis	25 - 40	blood plasma	[20]

Supplementary Table 2. L-Tryptophan concentrations of different blood serum samples and spiked samples (+ 25 µM L-Trp) thereof determined using quantitative HPLC with an estimated error of 5%.

medium	[L-Trp] (µM) in serum	[L-Trp] (µM) in spiked serum
human serum (MERCK)	20 ± 1.0	48 ± 2.0
steroid depleted human serum (SEQENS)	2.0 ± 0.1	32 ± 2.0
bovine calf serum (CYTIVA)	39 ± 2.0	65 ± 3.0

Supplementary Table 3. Mean fluorescence intensities in the spots of rotaxane **1** microarrays for L-tryptophan detection at varying concentrations. See also Supplementary Fig. 9.

intensity (a.u.)	control (1X PBS)	L-Trp				
concentration (M)		10^{-9}	10^{-8}	10^{-7}	10^{-6}	10^{-5}
before incubation with L-Trp	1.00 ± 0.06	1.00 ± 0.13	1.00 ± 0.13	1.00 ± 0.13	1.00 ± 0.08	1.00 ± 0.07
after incubation with L-Trp	0.92 ± 0.05	0.90 ± 0.11	0.78 ± 0.18	0.49 ± 0.09	0.34 ± 0.05	0.26 ± 0.06

Supplementary Table 4. Fluorescence intensities of rotaxane **1** or CB8•MDAP microarrays in the absence and presence of indole and memantine. See also Supplementary Fig.10.

intensity (a.u.)	control	indole	Mem	Mem (CB8•MDAP)
before incubation with analyte	1.00 ± 0.08	1.00 ± 0.15	1.00 ± 0.15	1.00 ± 0.16
after incubation with analyte	0.94 ± 0.10	0.31 ± 0.06	0.91 ± 0.12	0.09 ± 0.08

Supplementary Table 5. Mean fluorescent intensities of the ratiometric rotaxane **1** microarray and reference DAP spots for the L-tryptophan detection. See also Supplementary Fig. 11.

intensity (a.u.)	DAP reference	rotaxane
before incubation with L-Trp	1.00 ± 0.20	0.38 ± 0.05
after incubation with L-Trp	1.00 ± 0.23	0.18 ± 0.05

8. Abbreviations

ACN	Acetonitrile
AdOH	1-Adamantanol
Arg	Arginine
β-CD	beta-Cyclodextrin
BSA	Bovine serum albumin
CB8	Cucurbit[8]uril
Cps	Counts per seconds
γ	Gyromagnetic constant
D	Translational diffusion constant
DAPI	4′,6-Diamidin-2-phenylindol
Δ	Diffusion delay
δ	Chemical shift, gradient pulse lenght
DAP	2,7-Diazapyrene
DBA	Direct binding assay
DBCO	Dibenzocyclooctyne
DEPT	Distortionless enhancement by polarization transfer
DPT^{2+}	2,7-Dimethyl-diazaphenanthrenium
DOSY	Diffusion ordered spectroscopy
ESI	Electrospray ionization
ECD	Electronic circular dichroism
e.g.	*Exempli gratia* = 'for example'
ε	Extinction coefficient
eq	Equivalent
EQ	Emission quenching
G	Guest
g	Gradient parameter
HEPES	4-(2-Hydroxyethyl)-1-piperazineethane-sulfonic acid
HPLC	High performance liquid chromatography
HTS	High-throughput screening
K_a	Binding constant
I	Emission intensity
I_o	Unattenuated signal intensity (DOSY)
IAA	Indole acetic acid
i.e.	*Id est* = 'that is'
λ	Wavelength
LC	Liquid chromatography
Lys	Lysine
$MDAP^{2+}$	2,7-Dimethylbenzo[*lmn*][3,8]phenanthrol-line-2,7-diium
MDL	4,4′-Diisocyanato methylendibenzol
$MDPP^{2+}$	2,9-Dimethyl peroperonium
MVE^{2+}	1,2-Dimethyl(4-pyridinyl)ethenium
m/z	Mass-to-charge ratio
μCS	Microchannel cantilever spotting
NHS	N-Hydroxysuccinimide
NMR	Nuclear magnetic resonance
PEG	Polyethyleneglycol
Phe	Phenylalanine
ref.	Reference
sccm	Standard cubic centimeter per minute
TCEP	Tris-(2-carboxyethyl)phosphine
TDL	Toluylene diisocyanate
TEG	Tetraethylene glycol
TFA	Trifluoroacetic acid
Trp	Tryptophan
UV-Vis	Ultraviolet–visible
wt%	Mass fraction (weight percentage)

9. References

1. Evans J.P., Ahn K., Klinman J.P. Evidence that dioxygen and substrate activation are tightly coupled in dopamine β-monooxygenase: Implications for the reactive oxygen species. *J. Biol. Chem.* **278**, 49691-49698 (2003).
2. Raichenok T.F., Litvinovskaya R.P., Zhabinskii V.N., Raiman M.E., Kurtikova A.L., Minin P.S. Synthesis and spectral and luminescence properties of new conjugates of brassinosteroids for immunofluorescence analysis. *Chem. Nat. Compd.* **48**, 267-271 (2012).
3. Marmorstein R.Q., Joachimiak A., Sprinzl M., Sigler P.B. The structural basis for the interaction between l-tryptophan and the escherichia coli trp aporepressor. *J. Biol. Chem.* **262**, 4922-4927 (1987).
4. *Handbook of biochemistry and molecular biology. Proteins-v. 1-3*, 3 ed. CRC Press (1976).
5. Vlasova N.N., Markitan O.V., Stukalina N.G. The adsorption of biogenic amines on the surface of highly dispersed silica from aqueous solutions. *Colloid J.* **68**, 384-386 (2006).
6. Nishino H., Kosaka A., Hembury G.A., Matsushima K., Inoue Y. The ph dependence of the anisotropy factors of essential amino acids. *J. Chem. Soc., Perkin Trans. 2*, 582-590 (2002).
7. Stang P.J., Cao D.H., Saito S., Arif A.M. Self-assembly of cationic, tetranuclear, pt(ii) and pd(ii) macrocyclic squares. X-ray crystal structure of [pt2+(dppp)(4,4'-bipyridyl).Cntdot.2-oso2cf3]4. *J. Am. Chem. Soc.* **117**, 6273-6283 (1995).
8. Hünig S., Groβ J., Lier E.F., Quast H. Über zweistufige redoxsysteme, xii1) synthese und polarographie von quartärsalzen der phenanthroline, des 2,7-diazapyrens sowie der diazoniapentaphene. *Liebigs Ann. Chem.* **1973**, 339-358 (1973).
9. Ellman G.L. Tissue sulfhydryl groups. *Arch. Biochem. Biophys.* **82**, 70-77 (1959).
10. Verch A., Hahn H., Krause E., Cölfen H., Börner H.G. A modular approach towards functional decoration of peptide–polymer nanotapes. *Chem. Commun.* **46**, 8938-8940 (2010).
11. Loftsson T., Saokham P., Sá Couto A.R. Self-association of cyclodextrins and cyclodextrin complexes in aqueous solutions. *Int. J. Pharm.* **560**, 228-234 (2019).
12. Li Y., Tang A.-G., Mu S. Hplc–fld determination of serum aromatic amino acids: Application in chronic kidney disease patients. *Clin. Chim. Acta* **412**, 1032-1035 (2011).
13. Zhong C., Hu C., Kumar R., Trouillet V., Biedermann F., Hirtz M. Cucurbit[n]uril-immobilized sensor arrays for indicator-displacement assays of small bioactive metabolites. *ACS Appl. Nano Mater.* **4**, 4676-4687 (2021).
14. Wirleitner B.*, et al.* Immune activation and degradation of tryptophan in coronary heart disease. *Eur. J. Clin. Investig.* **33**, 550-554 (2003).
15. Psychogios N.*, et al.* The human serum metabolome. *PLoS One* **6**, e16957 (2011).
16. Fonteh A.N., Harrington R.J., Tsai A., Liao P., Harrington M.G. Free amino acid and dipeptide changes in the body fluids from alzheimer's disease subjects. *Amino Acids* **32**, 213-224 (2007).
17. Konje V.C.*, et al.* Tryptophan levels associate with incident cardiovascular disease in chronic kidney disease. *Clin. Kidney J.* **14**, 1097-1105 (2020).
18. Weiss G., Schroecksnadel K., Mattle V., Winkler C., Konwalinka G., Fuchs D. Possible role of cytokine-induced tryptophan degradation in anaemia of inflammation. *Eur. J. Haematol.* **72**, 130-134 (2004).
19. Herrera-Van Oostdam A.S.*, et al.* Immunometabolic signatures predict risk of progression to sepsis in covid-19. *PLoS One* **16**, e0256784 (2021).
20. Ploder M.*, et al.* Accelerated tryptophan degradation predicts poor survival in trauma and sepsis patients. *Int. J. Tryptophan Res.* **3**, IJTR.S3983 (2010).